

Advanced High Porosity Ceramic Honeycomb Wall Flow Filters

Bilal Zuberi, James J. Liu, Sunilkumar C. Pillai, Jerry G. Weinstein
GEO2 Technologies, Woburn, MA, USA

Athanasios G. Konstandopoulos, Souzana Lorentzou, Chrysa Pagoura
Aerosol Particle Technology Laboratory, CPERI/CERTH, Thessaloniki, Greece

Copyright © 2007 SAE International

ABSTRACT

A new platform of advanced ceramic composite filter materials for diesel particulate matter and exhaust gas emission control has been developed. These materials exhibit high porosity, narrow pore-size distribution, robust thermo-mechanical strength, and are extruded into high cell density honeycomb structures for wall-flow filter applications. These new high porosity filters provide a structured filtration surface area and a highly connected wall pore space which is fully accessible for multi-phase catalytic reactions. The cross-linked microstructure (CLM™) pore architecture provides a large surface area to host high washcoat/catalyst loadings, such as those required for advanced multi-functional catalysts (4-way converter applications). Data from flow reactor and engine dynamometer studies conducted in house as well as at independent laboratories show low comparative pressure drop of the Composite filter materials versus standard industry powder-based ceramic filters (Cordierite and SiC). Filtration efficiency measurements have also been conducted using particle number concentration based methods, and high trapping efficiencies have been observed on steady state and transient cycles. These filters can be manufactured using GEO2's technology platform from a variety of oxide and non-oxide materials such as: Mullite, SiC and others.

INTRODUCTION

Diesel engines are known to achieve superior fuel efficiency, high torque output and longevity than like-sized gasoline engines. It is for that reason they have gained significant market share in light, medium and heavy duty markets around the world. In a world that is rapidly coming to terms with the need to reduce CO₂ emissions from the automotive sector, diesel engines are prominent choice because of their lower overall carbon-based emissions. However, due to the particularities of the compression ignition combustion processes, diesel engines post a challenge for the control of both harmful nitrogen oxides (NO_x) and toxic particulate matter (PM) in the tailpipe. [1-2]

Emission regulations around the world are tightening and forcing diesels to dramatically reduce PM and NO_x emissions. While improvements are being made in the engine control and combustion processes themselves, post-engine PM and NO_x emission control systems have become necessary to comply with the regulatory emission levels.

A diesel particulate filter (DPF) is a device designed to capture, store, and then regenerate PM emissions from diesel engines. Similarly, advanced catalytic converters are also used to reduce NO_x emissions in the tailpipe, and novel catalyst systems are now being developed that would combine the NO_x reduction functionality onto the DPF itself (in a multifunctional filter/4-way convert system). [3]

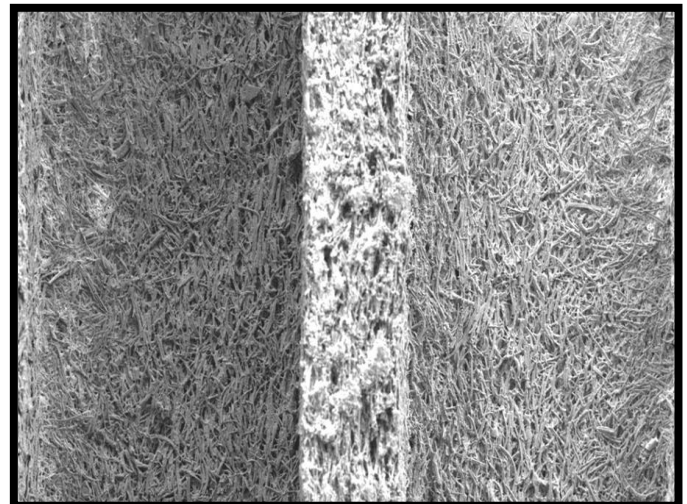


Figure 1: High resolution scanning electron micrograph of GEO2's Composite-M extruded honeycomb filter.

Diesel particulate filters were first developed more than twenty years ago to deal with the diesel particulate problem, particularly in heavy-duty applications. These DPFs were based on a modification to the pore structure of the existing powder-based cordierite ($2\text{MgO}\cdot 2\text{Al}_2\text{O}_3\cdot 5\text{SiO}_2$) ceramic used for automotive catalytic converter substrates. [4-5]. The porosity of the walls in the honeycomb was increased to allow gases to pass

through without much obstruction, but the particles were trapped in alternately plugged channels of the honeycomb (wall-flow design). The low cost extrusion process allowed for manufacturability and high surface area filtration. Subsequently, for robustness and durability reasons, a powder-based SiC ceramic chemistry was developed that was more expensive to produce but provided better resistance to melting during uncontrolled PM regeneration events. [6-8]

As the emission control regulations have tightened, there is a need for improved DPF materials that would have lower backpressure, high filtration efficiency (especially for nano-particles), required robustness and durability, and could be manufactured at scale. Additionally, for integration of multiple catalyst functionalities onto the DPF, high porosity (>60%) has been desirable, which has not been possible to achieve in other filter materials. Several new filter materials have been introduced, but they have not met the one or more of the criteria listed above and have been found to be compromised. [9-20].

RESULTS

GEO2 has developed a unique platform of high porosity composite DPF materials that combines the low cost extrusion processes used to manufacture high cell density honeycombs with a novel cross-linked microstructure (CLM) in the DPF walls. This microstructure produces a combination of high strength at high porosity and high material permeability for a given pore size distribution. The scanning electron micrograph (SEM) of composite honeycomb is shown in Figure 1. While several specific oxide and non-oxide chemistries have been extruded into honeycombs with the novel cross-linked wall microstructure (such as silicon carbide, cordierite and alumina), this paper will focus only on the composite Mullite (Composite-M) material. [21]

PHYSICAL AND MECHANICAL PROPERTIES

The high porosity composite wall-flow honeycomb DPFs are manufactured using standard industry extrusion equipment. Depending on the application, 100-300 cells per square inch (cps) honeycombs can be extruded with wall thicknesses ranging from 10 mils (0.25 mm) to 20 mils (0.50 mm). These filters can be made with porosities ranging from 50% to 75%, and pore-sizes from 9 μm to 30 μm.

For all results shown below, the following configuration was used:

- 5.66"x6" (144 mm x 152 mm) – 4-segment wall-flow design
- Nominal 200 cps, 18 mil (0.43 mm) wall thickness

Table 1 provides basic properties of Composite-M filters used for measurements presented in this paper.

Table 1: Physical and mechanical properties of Composite-M filters with commercial Cordierite and SiC filters.

	Composite-M (GEO2 200/18)	Cordierite (Corning CO 200/12)	Si-SiC (NGK 300/12)
Porosity (%)	67%	47%	48%
Avg Pore-diameter (μm)	15	13	13
Crush Strength (axial) (psi)	1000	1168	1426
MoR [6x4x40mm] (MPa)	8.6	2.2	9.4
E Modulus (GPa)	7.8	4.8	13.3
Max Op. Temp (°C)	>1500°	~1350°	>1600°
CTE [200-800°C]/(K)	4.3×10^{-6}	0.7×10^{-6}	4.4×10^{-6}
TSP (w/o conductivity)	187	275	142
Specific heat (J/g°C)	1.025	1.18	1.07

PERFORMANCE TESTING

As a diesel particulate filter, key metrics used in evaluation of performance in application include filtration efficiency [22] and backpressure over steady state and transient driving cycles, as well as thermal durability and performance during controlled and uncontrolled regenerations. The following filters were tested:

Material	Identification	Cpsi/wall thickness	Dimensions
Composite-M	Filter A	200/18	Ø141 mm x 153 mm
Cordierite	Filter B	200/12	Ø144 mm x 152 mm
SiC-based	Filter C	300/12	Ø144 mm x 153 mm

ENGINE AND EXHAUST SETUP

A common-rail diesel engine (displacement 1.9L, rated power 60 KW), coupled to a servo-controlled dynamometer was used. The engine exhaust system was able to host several DPFs of different dimensions as well as a DOC upstream of the DPF. Special built exhaust modules for particle and gas sampling were placed upstream of the DOC and the DPF and

downstream of the DPF. The system had the capability to by-pass the exhaust flow at the beginning of the test to allow the engine to reach steady state operation conditions (Figure 2). It also incorporated the necessary pressure and temperature sensors as well as a hydrocarbon port injection system (in-house development) for DPF regeneration purposes.

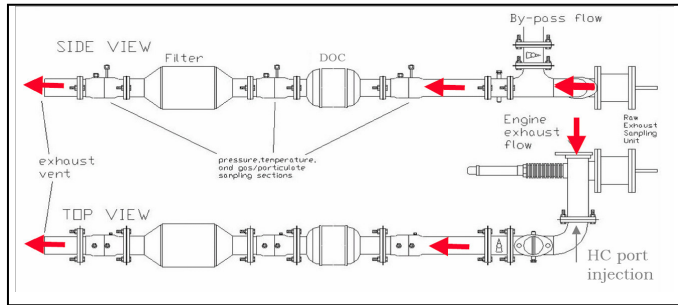


Figure 2: Exhaust setup for particle measurements and DPF testing

PARTICLE MEASUREMENT INSTRUMENTATION

PM filtration efficiency was monitored by measurements upstream and downstream of the DPF using a suite of analytical instrumentation for particle number based concentration (Figure 3), including:

1. Electric Low Pressure Impactor (ELPI). This is an aerodynamic method based instrument. It measures in real-time particle size and number concentration of particles. It is connected to a 2-stage mini-diluter and provides the number concentration of particles with size in the range of 30 nm to 8 μm .
2. Condensation Particle Counter (Standalone CPC). This is a laser based particle counter. It is connected to a 3-stage mini-diluter system and it is used for real-time total particle number concentration measurements.
3. Scanning Mobility Particle Sizer (SMPS). This is an electrical mobility method based instrument. It is also connected to a 3-stage mini diluter system and consists of a Differential Mobility Analyser (DMA) combined with an Ultrafine Condensation Particle Counter (U-CPC). It provides the number concentration of each particle size in the range of 10 to 430 nm. The integration of the number concentration over the entire particle size range provides the total particle concentration. SMPS can also be set to continuously measure (in real time) particle number concentration at a specific particle size (e.g. 80 nm).

Each instrument sampled the pre- and post- DPF diesel exhaust through a heated two-stage mini-diluter system (190 °C), with a dilution ratio of 90.

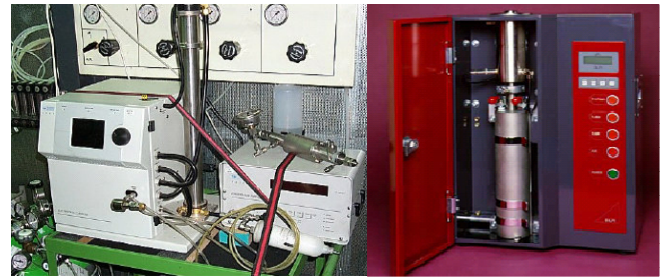


Figure 3: ELPI, CPC and SMPS particle measurement systems

STEADY STATE ENGINE OPERATION MEASUREMENTS

During engine operation, soot from the diesel exhaust stream is captured by the DPF. During this soot loading, it is important for the filtration efficiency of the filter to always remain high. As the soot accumulates on the DPF, the pressure drop across the DPF increases, thus increasing engine backpressure. High engine backpressure will significantly reduce engine power output and performance. Therefore, lower DPF pressure drop is desired.

Initial filtration efficiency and soot-loaded backpressure measurements were done under steady state soot loading conditions with the engine operating at 1500 rpm with 45 Nm torque load. Under such controlled conditions, the differences in performance between Composite-M filters, and the benchmark Cordierite and SiC filters are obvious.

As shown in Figure 4, the y-axis indicate the PM filtration efficiency and the pressure drop, while the x-axis represents the challenge soot mass load (actual soot mass load that would be collected on an absolute filter (100% efficiency) divided by the actual surface area of the DPF under examination). The initial filtration efficiency of Composite-M filters is greater than 80% and quickly rises to more than 99% at less than 0.2 g/m^2 of soot loading. It can be observed that Cordierite and SiC-based filters demonstrate a similar PM filtration efficiency but cause a larger increase in backpressure as a function of soot loading compared to Composite-M filters. At similar filtration velocities (approximately 1.80 cm/s), Composite-M filter reaches a maximum backpressure of 16 mbars, while Cordierite filter reaches a maximum backpressure of 27 mbars at a soot loading of 5 g/m^2 . At a similar filtration flow velocity, SiC filter would also be expected to exhibit a higher backpressure than Composite-M filter.

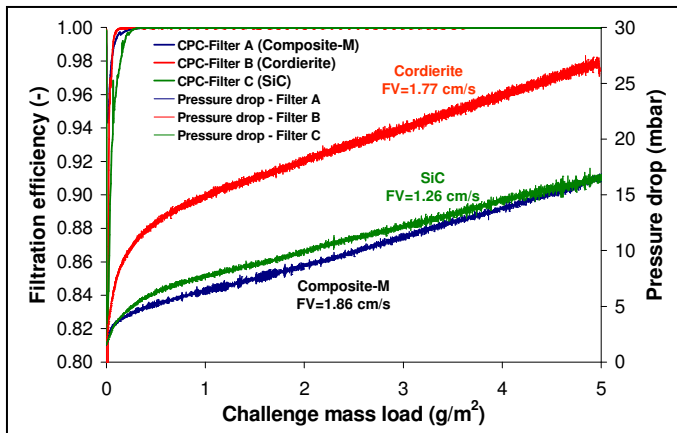


Figure 4: Evolution of filtration efficiency and backpressure as a function of soot loading in Composite-M, Cordierite and SiC-based filters. FV=filtration velocity.

In order to better characterize the PM filtration efficiency of Composite-M high porosity filters, size specific filtration efficiency was obtained by simultaneously monitoring PM concentrations upstream and downstream of the DPF using an SMPS system (Figure 5(a)). Each scan lasted 135 seconds, and as can be observed, Composite-M filters exhibit high initial filtration efficiency for all particle sizes of interest, and nano-particle filtration efficiency continues to improve as a function of time.

Figure 5(b) shows size-specific filtration efficiency measured using an SMPS at three different filtration flow velocities. It is noted that the filtration efficiency remains high over a wide range of filtration flow velocities though the maximum penetrating diameter shifts slightly towards smaller sizes as filtration flow velocity increases.

Interestingly, there is a shift of the mean particle diameter to higher values for the soot particles downstream of the DPF. This fact reveals that filtration is diffusion controlled with the smaller particles filtered with higher efficiency. [23-24]

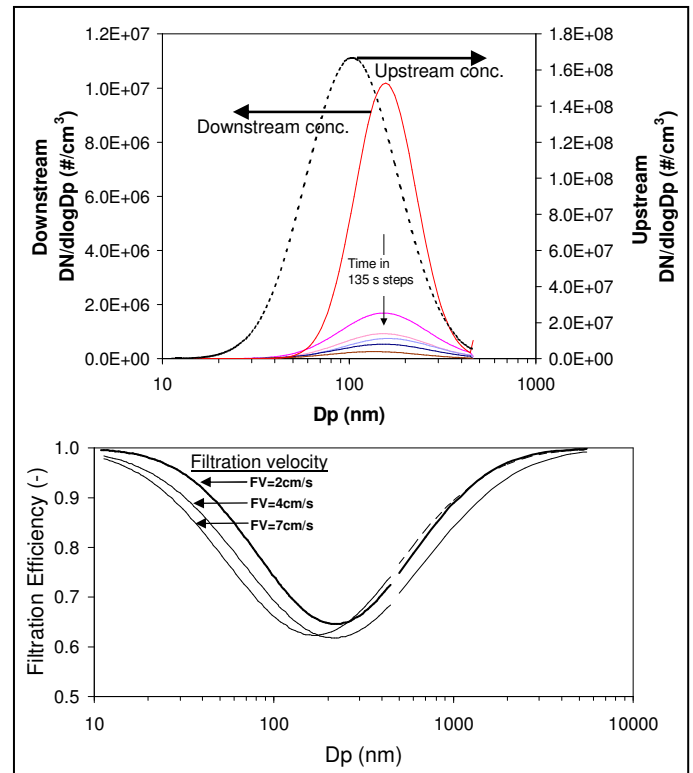


Figure 5: (a) PM concentrations measured upstream and downstream of the Composite-M DPF using SMPS. Multiple 135s scans shown. (b) Size-specific initial filtration efficiency measured at different filtration flow velocities (FV): 2 cm/s, 4 cm/s, and 7 cm/s.

TRANSIENT ENGINE OPERATION MEASUREMENTS

New European Driving Cycle (NEDC) consists of four repeated ECE-15 driving cycles and an Extra-Urban driving cycle, or EUDC. The NEDC represents the typical usage of a car in Europe. The New European Driving Cycle (NEDC) was employed as representative of engine transient operation. Figure 6 provides the evolution of engine speed and torque during the NEDC.

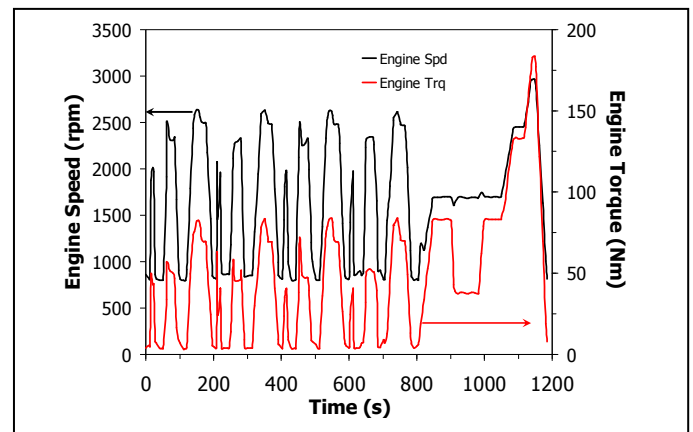


Figure 6: Engine speed and torque during the NEDC

With the exception of the SMPS all other particle analyzers (CPC and ELPI) are able to monitor the exhaust soot particles in real time (time resolution of 1 s) during transient engine operation. The SMPS can also be set to continuously measure particle number

concentration but only for a given particle size (e.g. 80 nm) denoted as SMPS-80.

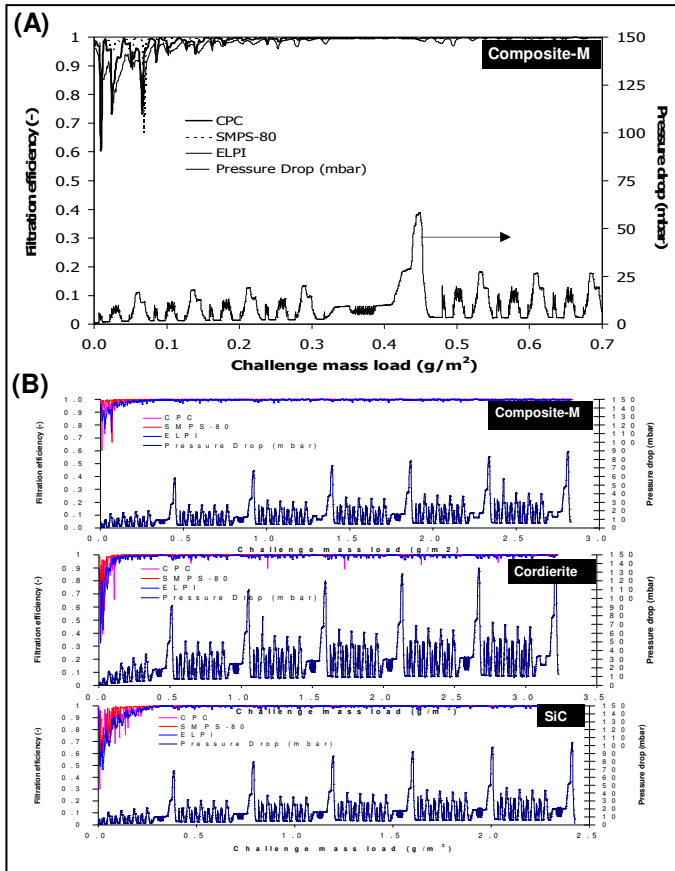


Figure 7: (a) Composite-M filter performance over NEDC Cycle (b) Filter performance for Composite-M, Cordierite and SiC, over multiple (6) NEDC driving cycles.

We tested Composite-M, Cordierite and SiC-based filters over multiple NEDC cycles to evaluate the performance of these filters under transient conditions. Figure 7a shows the performance of Composite-M filter over an NEDC cycle. Figure 7b shows the performance of Composite-M, Cordierite and SiC-based filters in terms of backpressure and filtration efficiency during multiple NEDC cycles.

It can be seen in Figure 7a that Composite-M filters exhibit high filtration efficiency over a range of filtration velocities over the transient conditions during the NEDC cycle. Figure 7b shows the data obtained for Cordierite and SiC-based filters. It can be observed that after 6 NEDC cycles, Composite-M filter has a maximum backpressure of 90 mbar which benchmarked filters have higher backpressure.

SOOT REGENERATION STUDIES

During operation, PM (soot) is collected inside the inlet channels of the DPF and backpressure continues to build up as a function of the thickness of soot cake layer. When a certain threshold of soot loading onto the filter is reached, the filter needs to regenerate (combust) the accumulated soot into CO₂. This exothermic reaction takes place when the temperature inside the filter is

raised to approximately 550°C for a bare filter, or as low as 300°C in the presence of a catalyst. During normal operation of a DPF, the engine periodically monitors the backpressure in the DPF and when the threshold level is reached, the exhaust temperature is raised to burn off the accumulated soot.

One way to raise the exhaust temperature is by varying the engine control parameters. Use of post injection of fuel in conjunction with an upstream DOC is a commonly employed strategy. The fuel combusts upon contact with the precious metal catalysts on the DOC, thereby raising the temperature of the downstream filter.

A post-injection regeneration technique was used to probe Composite-M filter for its soot balance temperature, performance during controlled regenerations, and resistance to thermal shock and large exothermic events during uncontrolled regeneration.

SOOT BALANCE POINT

Soot Balance Point is the temperature at which a filter is in equilibrium with its soot mass, i.e. the temperature at which the rate of soot loading is equal to the rate of soot regeneration. Under steady state conditions of 1500 rpm and 45 Nm torque, the soot balance point of a bare Composite-M 5.66"x6" filter was determined to be 560°C (Figure 8).

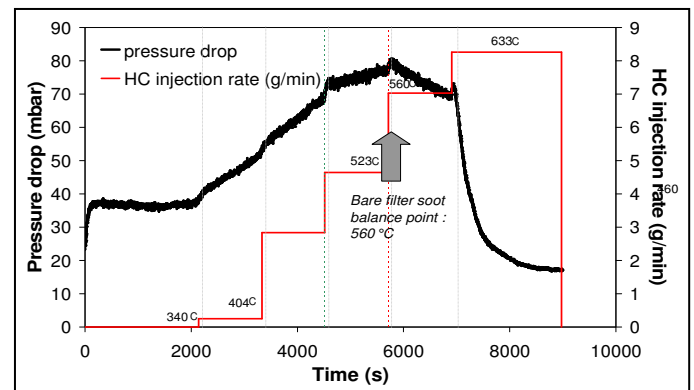


Figure 8: Soot balance point of a bare Composite-M filter determined using pre-DOC post-injection soot regeneration.

FILTRATION EFFICIENCY DURING REGENERATION

Filtration efficiency monitoring can also be performed under filter regeneration conditions. For the regeneration tests the DPFs were first loaded with soot up to a moderate soot mass load. Then a DOC was placed upstream of the DPF. In order to increase the exhaust temperature, a predefined quantity of engine fuel was injected upstream of the DOC with the engine operating at a steady state condition of 1500 rpm, 75 Nm.

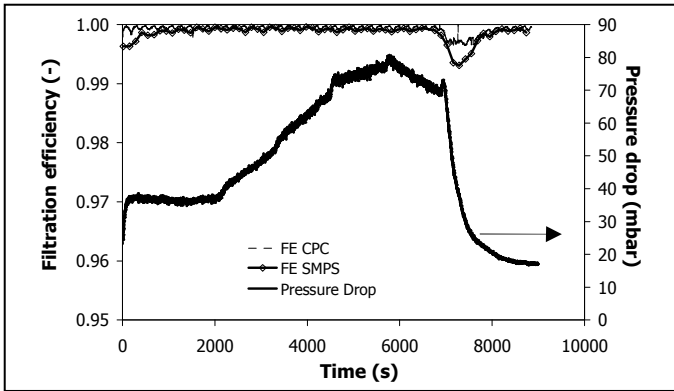


Figure 9: Filtration efficiency and backpressure during controlled regeneration using post-injection upstream of a DOC.

Figure 9 shows the filtration efficiency of a Composite-M filter as measured using CPC and SMPS-80. It can be seen that even during regeneration, when the backpressure exerted by the filter drops rapidly, the filtration efficiency remains higher than 99%. No soot blow-off or blow-by was observed [25-26]

CONTROLLED REGENERATION

The development of pressure drop during controlled soot oxidation under a 3°C/min temperature ramp, in a 10% O₂ exhaust stream for a Composite-M and a standard SiC filter is shown in Figure 10. Figure 11 depicts the soot oxidation rate, obtained by integration of the CO and CO₂ evolution during the controlled regeneration of the filters. Both the pressure drop and oxidation rate data demonstrate that controlled regeneration proceeds at the same rate on both filters.

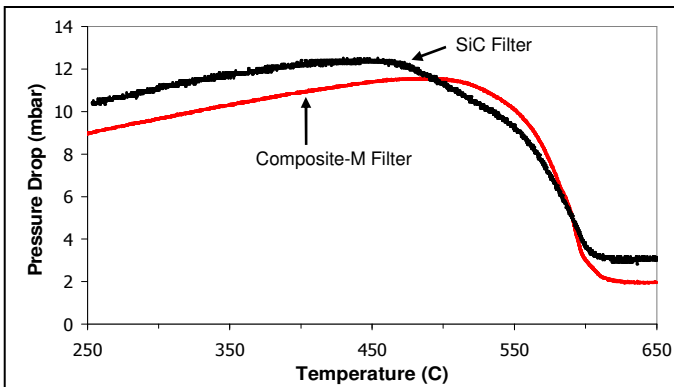


Figure 10. Pressure drop evolution of uncoated Composite-M and standard SiC filters during soot oxidation.

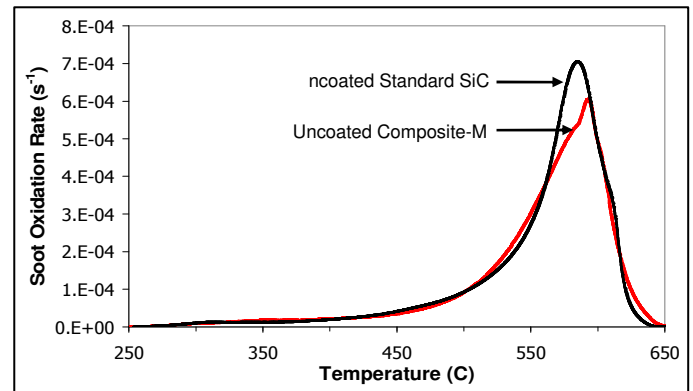


Figure 11. Soot oxidation rate of uncoated filters.

UNCONTROLLED REGENERATION

While the typical filter regeneration process is performed under controlled conditions, real world applications can result in worst case scenarios where the filter reliability and performance is severely tested. At high soot loadings, uncontrolled regeneration can lead to high maximum temperatures inside the filter, as well as the generation of large radial and axial thermal gradients leading to thermal shock. Severe regeneration tests are commonly used to predict the reliability of DPFs.

Severe regeneration tests were performed on a Composite-M filter using the following drop-to-idle protocol:

1. Load predefined soot mass load a DOC upstream of filter
2. Place DOC upstream of filter
3. Set engine to the steady state operation point of 1500 rpm and 75 Nm BMEP (corresponding to 340°C filter inlet temperature)
4. Engine exhaust temperature is increased to 650°C with the means of HC port injection upstream of the DOC
5. Drop to idle.

Composite-M-filter was tested for survivability in consecutive uncontrolled regenerations at two different soot mass loadings: 10 g/m² (~7 g/liter) and 15 g/m² (~10 g/liter). After loading the filter with a pre-determined mass of soot, 9 thermocouples were inserted into the filter to probe the thermal gradients observed in the filter. The location of the thermocouples inside the filter is shown in Figure 12.

Figure 12(b) shows that the maximum temperature approached 1100°C, and large thermal gradients were generated inside the Composite-M filter during severe uncontrolled regenerations. Composite-M filter survived the severe thermal shock tests and continued to perform with high filtration efficiency. Initial permeability of the filter was also measured at 6x10⁻¹³ m², and that remained unchanged, indicating the absence of any crack generation during the thermal shock tests.

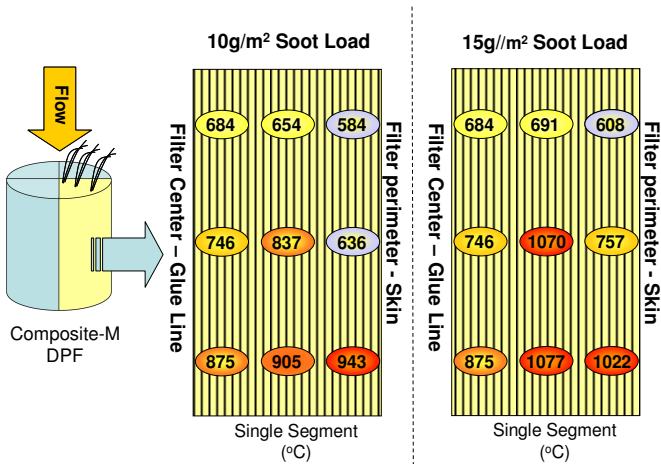


Figure 12: Maximum temperatures observed during uncontrolled regeneration in Composite-M filter at (a) 10g/m² and (b) 15 g/m².

REGENERATION RELATED THERMAL CYCLING/FATIGUE

A typical DPF undergoes hundreds of regeneration cycles during its lifetime in operation. This thermal cycling can lead to fatigue and weakening of the ceramic DPF. In order to ensure reliable performance of the DPF after hundreds of controlled regenerations, a simulated thermal cycling test was set up and Composite-M filter evaluated for resistance to thermal fatigue.

A heater-blower assembly operating at 38 CFM flow rate was setup to heat a Composite-M filter from 350°C to 750°C at a rate of 100°C/min and then cooled back down at 200°C/min. The exact cycle is shown in Figure 13.

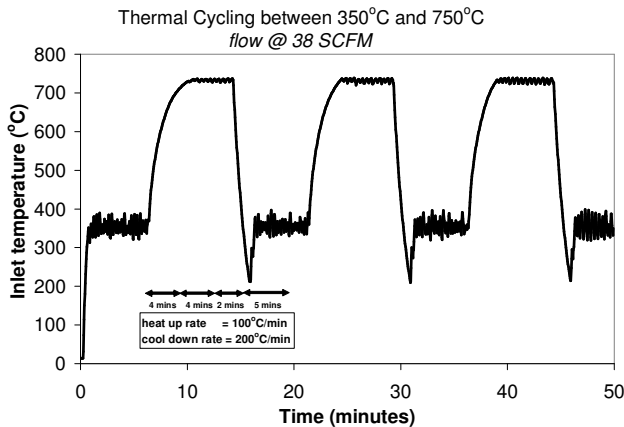


Figure 13: Thermal cycle used to simulate controlled regenerations

Composite-M filter was evaluated for structural integrity and mechanical properties after being subjected to 1000 cycles representing controlled regenerations. No physical defects or cracks were detected and the MoR and E-modulus values remain unchanged.

CATALYST PERFORMANCE

Catalyzed DPFs are expected to reduce the soot oxidation temperature and to potentially allow continuous soot regeneration at given engine conditions. Most light duty diesel engine applications use catalyzed DPFs in

their new engine platforms. There are two primary types of oxidation catalysts used in DPFs [27]: Precious metals, such as platinum, are used to facilitate indirect soot oxidation via NO/NO₂ reactions with soot. Redox materials, such as CeO₂, are used to facilitate direct soot oxidation by reducing the temperature required for O₂+soot reactions. In addition, 4-way filters that combine the PM and NOx removal capability onto a single filter, such as SCR on filter or NOx storage catalyst on DPF, require high washcoat/catalyst loadings to enable DeNOx functionality. [28]

As shown in Figure 1, Composite-M filter has a unique cross-linked microstructure which is obtained using proprietary chemistry and standard honeycomb extrusion processes. The interconnected pore-architecture inside the wall enables the porosity of the wall to be 'available' for storing washcoat and catalyst in catalyzed filter or multifunctional filter applications.

The high 'available' and open porosity provides two distinct advantages in catalyzed filter applications:

1. Lower increase in backpressure as a function of washcoat/catalyst loading
2. Better dispersion of washcoat and catalyst throughout the filter wall

IN-DIRECT SOOT OXIDATION

In order to investigate catalyst coating impact on backpressure and conversion efficiency, a 200/18 Composite-M filter was coated with 3 g/m² Pt (Platinum) catalyst on Al₂O₃. A commercially coated 200/12 cpsi SiC filter with 3 g/m² Pt catalyst on Al₂O₃ was also obtained.

Figure 14 shows the Pt elemental maps on the walls of the Composite-M and SiC filters. The Pt distribution on the Composite-M filter appears more homogeneous due to the higher porosity of this filter.

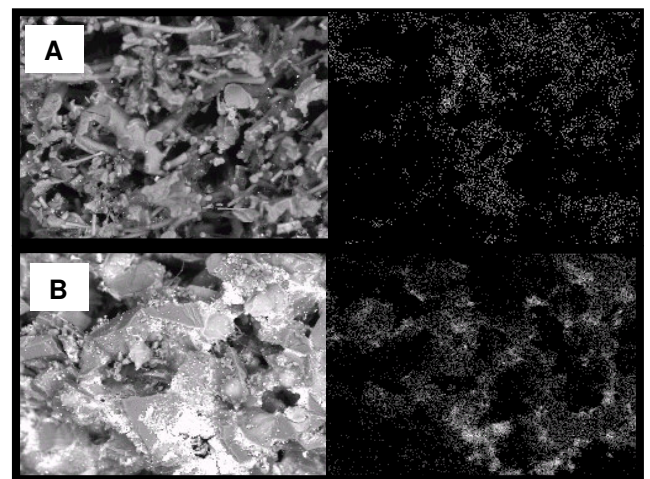


Figure 14. SEM images and Pt elemental maps of (a) a Composite-M and (b) a SiC filter coated with precious metal.

Figure 15 shows the evolution of backpressure on a bare Composite-M filter, a coated Composite-M filter, and a

coated SiC filter as a function of soot challenge mass load. Soot was loaded at 1500 rpm / 45 Nm with a filtration flow velocity of 2 cm/s and the exhaust temperature during loading at 250°C.

As can be seen, the washcoat/catalyst induced increase in backpressure is minimal on Composite-M filter compared to a commercially coated SiC filter. In addition, it is also noted that the shape of the curve is flat, with a lack of the prominent 'bend' observed on commercial SiC and cordierite filters that is associated with dramatic changes in permeability due to initial deep-bed filtration.

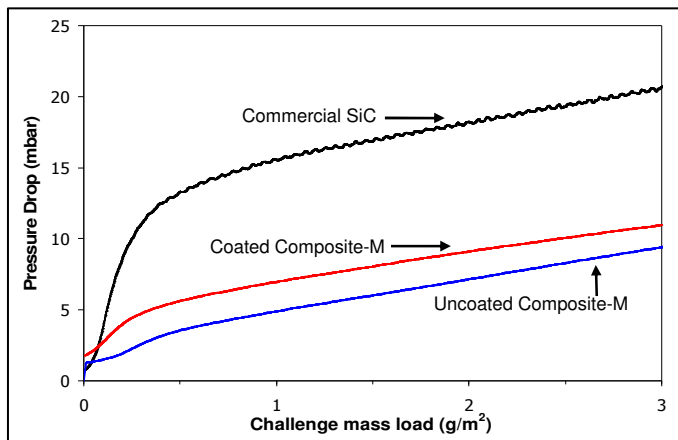


Figure 15: Evolution of backpressure on coated filters as a function of soot challenge mass load.

The NO/NO₂ assisted soot oxidation rate as a function of inlet gas temperature was measured on the coated Composite-M and SiC filters by exposing the filters to a gas stream containing 10% O₂ and 300 ppm NO. The black solid line in Figure 16 indicates the performance of a bare Composite-M filter. Soot oxidation activity was observed to peak at approximately 600°C. Just to check, pure O₂ stream without NO was exposed to a coated Composite-M filter and similar activity was observed. This indicated that our test was well set up to probe indirect soot oxidation via the NO₂ reaction mechanism.

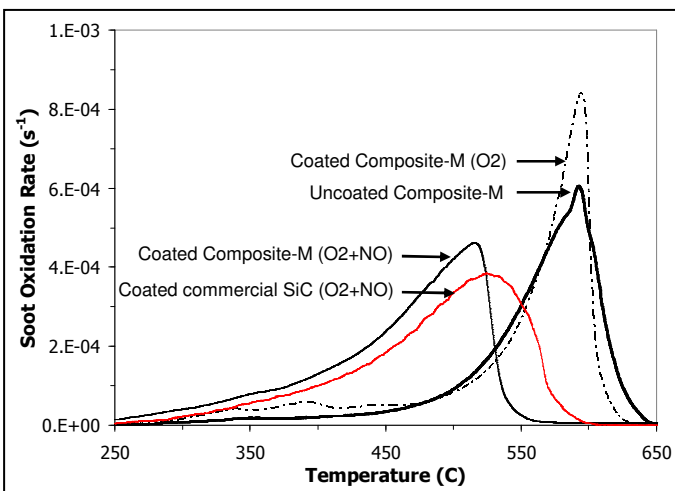


Figure 16: NO/NO₂ assisted soot oxidation rate on Pt coated filter samples

The red (dash) and the black (dash) lines indicate the soot oxidation activity for coated commercial SiC filter and coated Composite-M filter, respectively. As can be seen, the maximum soot oxidation activity was observed at a lower temperature on Composite-M filter than commercial SiC filter. We attribute this performance advantage to the lower thermal mass and better dispersion of catalyst on Composite-M filter.

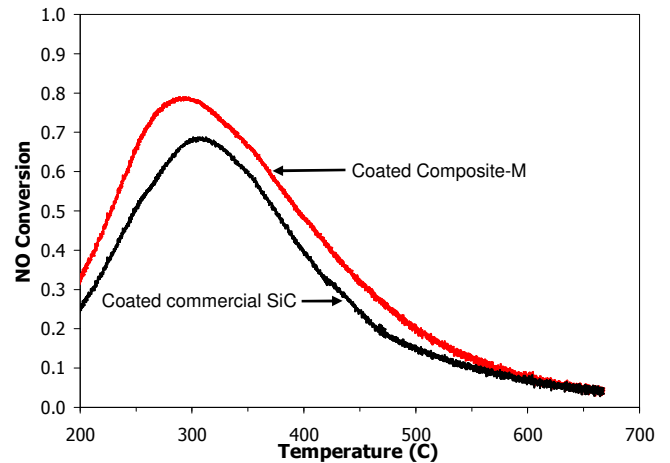


Figure 17. NO/NO₂ conversion as a function of the temperature for Pt-coated Composite-M and a commercial SiC filter.

Figure 17 shows the NO/NO₂ conversion rate observed in Composite-M filter versus commercial coated SiC filter.

DIRECT SOOT OXIDATION

Coating of the Composite-M filter with base metal catalysts (with oxygen storage capacity) was subsequently investigated. A 200/18 Composite-M filter was coated with a base metal catalyst and for comparative purposes a standard SiC 300/12 cpsi filter was coated with the same catalyst. Figure 18 depicts the catalyst distribution (white regions), unoccupied pore space (dark regions) and solid material (grey region) obtained from SEM images (backscatter mode). Interestingly enough the Composite-M filter contains about three times higher amount of catalyst than the SiC filter (202 g/liter vs. 78 g/liter) but still exhibits a large amount of unoccupied pore space, which results in a significantly lower pressure drop during soot loading as seen in Figure 19. In 4-way filter applications, such as an SCR-filter or a LNT-filter, high washcoat/catalyst loadings are required to achieve high conversion efficiencies, and filter materials, such as Composite-M, that exhibit high porosity and permeability despite significant washcoat/catalyst loadings are considered more suitable.

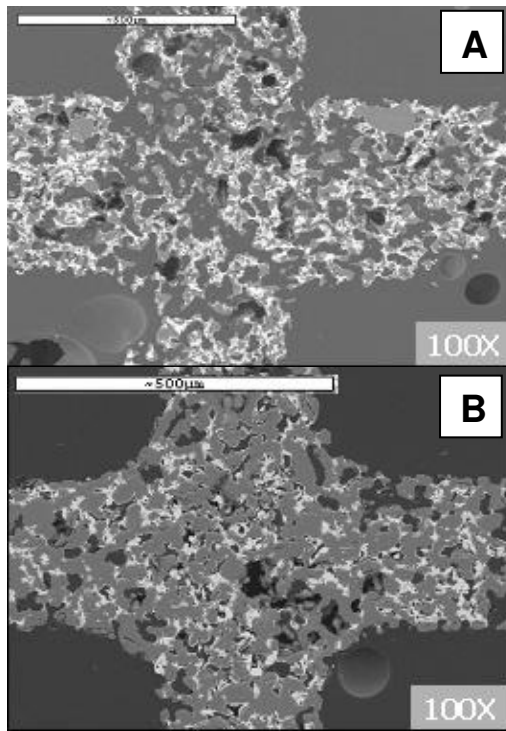


Figure 18. SEM images of (a) Composite-M and (b) SiC filter coated with base metal oxides. Composite-M had 3X loading as compared to SiC filter.

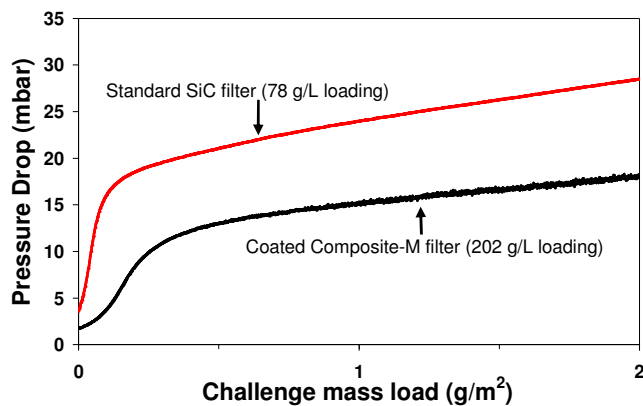


Figure 19. Pressure drop evolution of coated with base metal oxides filters.

Figures 20 and 21 depicts the positive effect that a direct soot oxidation catalyst can have when coated on the Composite-M filter. While the study of direct soot oxidation catalyst coatings on the Composite-M filter is on going, these results illustrate the potential advantages that can be realized in terms of low pressure drop, high catalyst loads and appreciable soot reactivity. The rational design and optimization of catalyst coatings on Composite-M structures will further benefit from applications of “Digital Materials” [29-30] approaches, already under way. Some preliminary reconstructions of fibrous walls are shown in Figure 22.

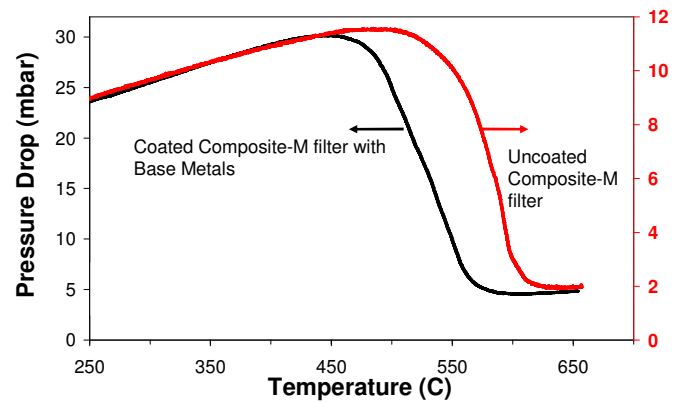


Figure 20. Comparison of the pressure drop evolution of an uncoated vs. a base metal coated Composite-M filter during soot oxidation.

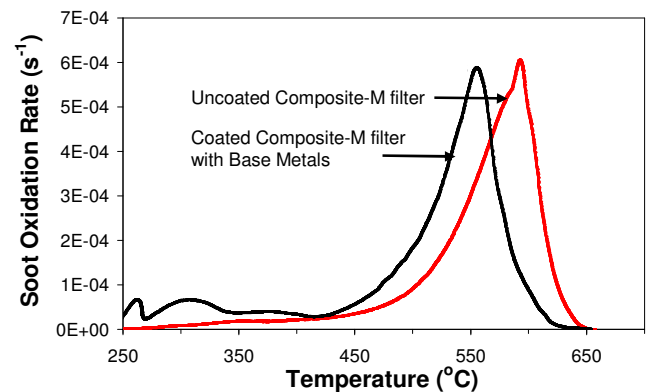


Figure 21. Comparison of the soot oxidation rate of an uncoated vs. a base metal coated Composite-M filter.

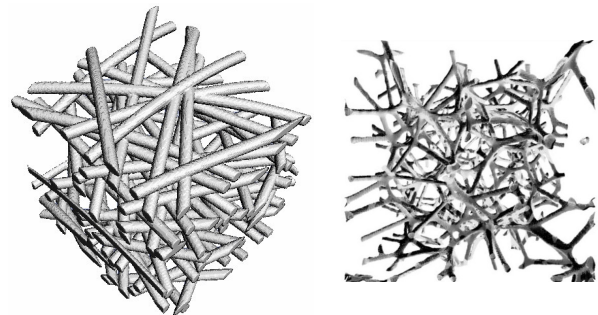


Figure 22. Computer reconstruction of fibrous porous structures

CHEMICAL STABILITY/ASH RESISTANCE

A diesel particulate filter is exposed to a variety of chemical species during the catalyst coating process or in operation that could interact unfavorably with the filter material. [31] These chemicals could originate in the diesel fuel itself, such as the sulfur content in the fuel, in the ash deposited from the burnt lubricant oil, or from wear and tear of the engine components itself. To address the chemical stability of Composite-M material when exposed to chemical/ash components, filter samples were immersed in concentrated solutions exposed to the following chemicals at 1000°C for 5 hours: Zinc nitrate, Cerium nitrate, Sodium hydroxide, Sulfuric acid, Engine Oil, Sodium chloride, and Potassium nitrate. SEM images of the reference Composite-M filter and ash exposed filter samples are shown in Figure 23.

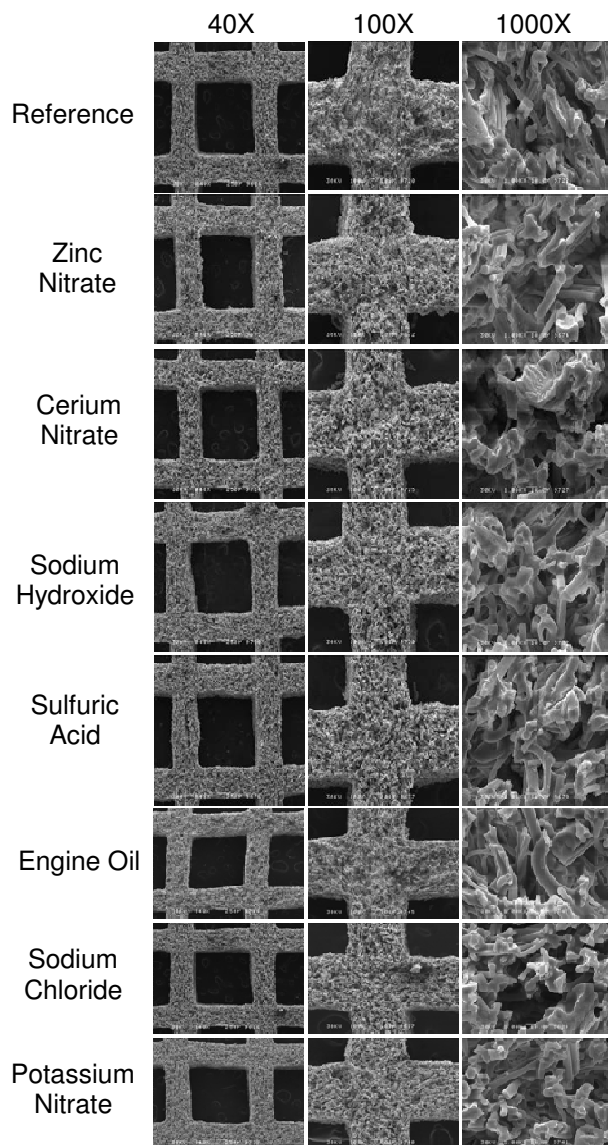


Figure 23: SEM images of Composite-M filters after exposure to ash constituents at 1000°C for 5 hours.

No visual or mechanical degradation, adhesion, pitting or melting of the filter material was observed. Additionally, no degradation of strength (measured using MoR) was observed.

Similar measurements were also conducted by exposing the filter to a mixture of commonly known ash constituents (e.g. CaO, P₂O₅, ZnO, MgO, Fe₂O₃, Na₂O) at temperatures between 1000°C to 1400°C for 1 hour. Around 1100°C ash adhesion and initial ash sintering was observed on the filter wall surface, without degradation of the filter structure. Pitting of the ceramic occurred at temperatures exceeding 1300°C.

CONCLUSION

GEO2 Technologies has developed high porosity composite materials with unique cross-linked microstructure for use in extruded honeycomb wall flow diesel particulate filters. These filters demonstrate high filtration efficiency and low backpressure while

maintaining structural robustness and mechanical/chemical durability required in DPF applications. These filters enable the application of catalyzed DPF, close-coupled DPF and multi-functional filters where deNO_x capability is provided onto the filter itself. The use of these composite provide potential for flexibility in design and size/cost reduction in emission control systems for various on-road and off-road applications.

ACKNOWLEDGMENTS

We wish to thank contributing team members at GEO2 Technologies, including Adam Wallen, Art O'Dea, Fredrick Porter, Jen Randall, Jim Marshall, Ken Donahue, Kyle Smith, Leonard Newton, Noah Loren, Rachel Dahl, Rob Lachenauer and Robert Miller. The assistance from the members of the Aerosol & Particle Technology Laboratory engine cell is also highly appreciated.

REFERENCES

1. Boland *et al.* Am J Physiol Lung Cell Mol Physiol 276: L604-L613 (1999)
2. Health Effects Institute, "Diesel Exhaust: A Critical Analysis of Emissions, Exposure, and Health Effects (A Special Report of the Institute's Diesel Working Group). Health Effects Institute, Cambridge, MA (1995)
3. Zuberi, B., "Multi-functional substantially fibrous mullite filtration substrates and devices", US 2006/0120937A1 (2006)
4. Murtagh *et al.*, "Development of a Diesel Particulate Filter Composition and Its Effect on Thermal Durability and Filtration Performance", SAE Paper 940235;
5. Merkel *et al.*, "Effects of Microstructure and Cell Geometry on Performance of Cordierite Diesel Particulate Filters", SAE Paper 2001-01-0193 (2001)
6. Ohno *et al.*, "Characterization of Sic-Dpf for Passenger Car", SAE Paper 2000-01-0185 (2000)
7. Hasimoto *et al.*, "SiC and Cordierite Diesel Particulate Filters Designed for Low Pressure Drop and Catalyzed, Uncatalyzed Systems", SAE Paper 2002-01-0322 (2002)
8. Majewski, A., *DieselNet Technology Guide*, <http://www.dieselnet.com>
9. Ichikawa *et al.*, "Material Development of High Porous Sic for Catalyzed Diesel Particulate Filters", SAE Paper 2003-01-0380 (2003)
10. Adler J., "Ceramic Diesel Particulate Filters", International Journal of Applied Ceramic Technology 2 (6), 429-439 (2005)
11. Li *et al.*, "Properties and Performance of Diesel Particulate Filters of An Advanced Ceramic Material", SAE Paper 2004-01-0955 (2004)
12. Ishizawa *et al.*, "IP Filter with DOC-integrated DPF for an Advanced PM Aftertreatment System (1): A

- Preliminary Evaluation*", SAE Paper 2007-01-0924 (2007)
13. Hiratsuka *et al.*, "The Latest Technology of Controlling Micro-Pore in Cordierite Diesel Particulate Filter for DPNR System", SAE Paper 2004-01-2028 (2004)
 14. Miller *et al.*, "Design, Development and Performance of a Composite Diesel Particulate Filter", SAE Paper 2002-01-0323 (2002)
 15. Shinozaki *et al.*, "Trapping Performance of Diesel Particulate Filters", SAE Paper 900107
 16. Mayer *et al.*, "Passive Regeneration of Catalyst Coated Knitted Fiber Diesel Particulate Traps", SAE Paper 960138
 17. Pyzik and Li, "New Design of a Ceramic Filter for Diesel Emission Control Applications", *Int. J. Appl. Ceram. Technol.*, 2 [6] 440–451 (2005)
 18. Kojima *et al.*, "Developments of diesel particulate Filter systems with mesh laminated structures", *JSAE Review*, 20, 117-136 (1999)
 19. Nakamura *et al.*, "Exhaust Gas Filter and Method for Making the Same", US5322537
 20. Suzuki *et al.*, "Diesel Particulate Filter Apparatus", US5611832
 21. Zuberi, B., *Refractory Exhaust Filtering Method and Apparatus*, US 7211232 (2007)
 22. Konstandopoulos *et al.*, "Multi-instrumental Assessment of Diesel Particulate Filters", SAE Paper 2007-01-0313 (2007)
 23. Ohara *et al.*, "Filtration Behavior of Diesel Particulate Filters (1)", SAE Paper 2007-01-0921 (2007)
 24. Fukushima *et al.*, "New Approach for Pore Structure and Filtration Efficiency Characterization", SAE Paper 2007-01-1918
 25. Konstandopoulos A. G., and Johnson J. H., "Wall-Flow Diesel Particulate Filters-Their Pressure Drop and Collection Efficiency", SAE Tech. Paper No. 890405 (1989)
 26. Giechaskiel *et al.*, "Particle Measurement Program (PMP): Particle Size and Number Emissions Before, During and After Regeneration Events of a Euro 4 DPF Equipped Light-Duty Diesel Vehicle", SAE Paper 2007-01-1944 (2007)
 27. Konstandopoulos *et al.*, "Catalytic Filter Systems with Direct and Indirect Soot Oxidation Activity", SAE Tech. Paper 2005-01-0670 (2005)
 28. Miller *et al.*, "Effect of Catalyst Support Structure on Conversion Efficiency", SAE Paper 2000-01-0183 (2000)
 29. Konstandopoulos *et al.*, "Application of Digital Material Methods to Silicon Carbide Diesel Particulate Filters", SAE Tech. Paper 2007-01-1131, (2007)
 30. Vlachos N. D., Konstandopoulos A. G., "Digital Materials Methods for DPF development", SAE Tech. Paper 2006-01-0260 (2006)
 31. Sappok *et al.*, "Detailed Chemical and Physical Characterization of Ash Species in Diesel Exhaust Entering Aftertreatment Systems", SAE Paper 2007-01-0318

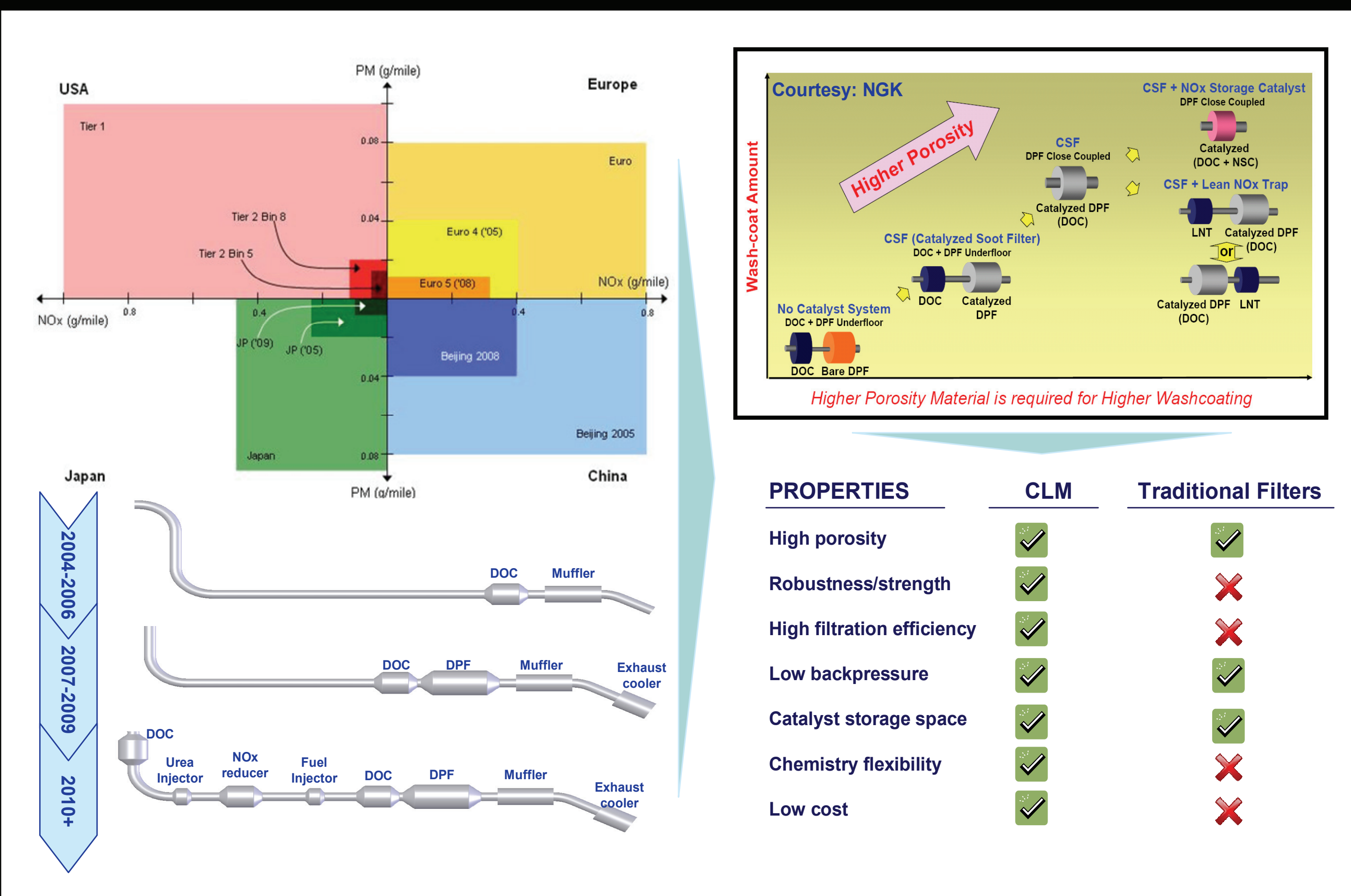
CONTACT

Bilal Zuberi has a Ph.D in physical chemistry from the Massachusetts Institute of Technology (MIT). He is a co-founder and Vice President of Product Development for GEO2 Technologies. 12-R Cabot Road, Woburn, Massachusetts 01801, USA (bzuberi@geo2tech.com, <http://www.geo2tech.com>)

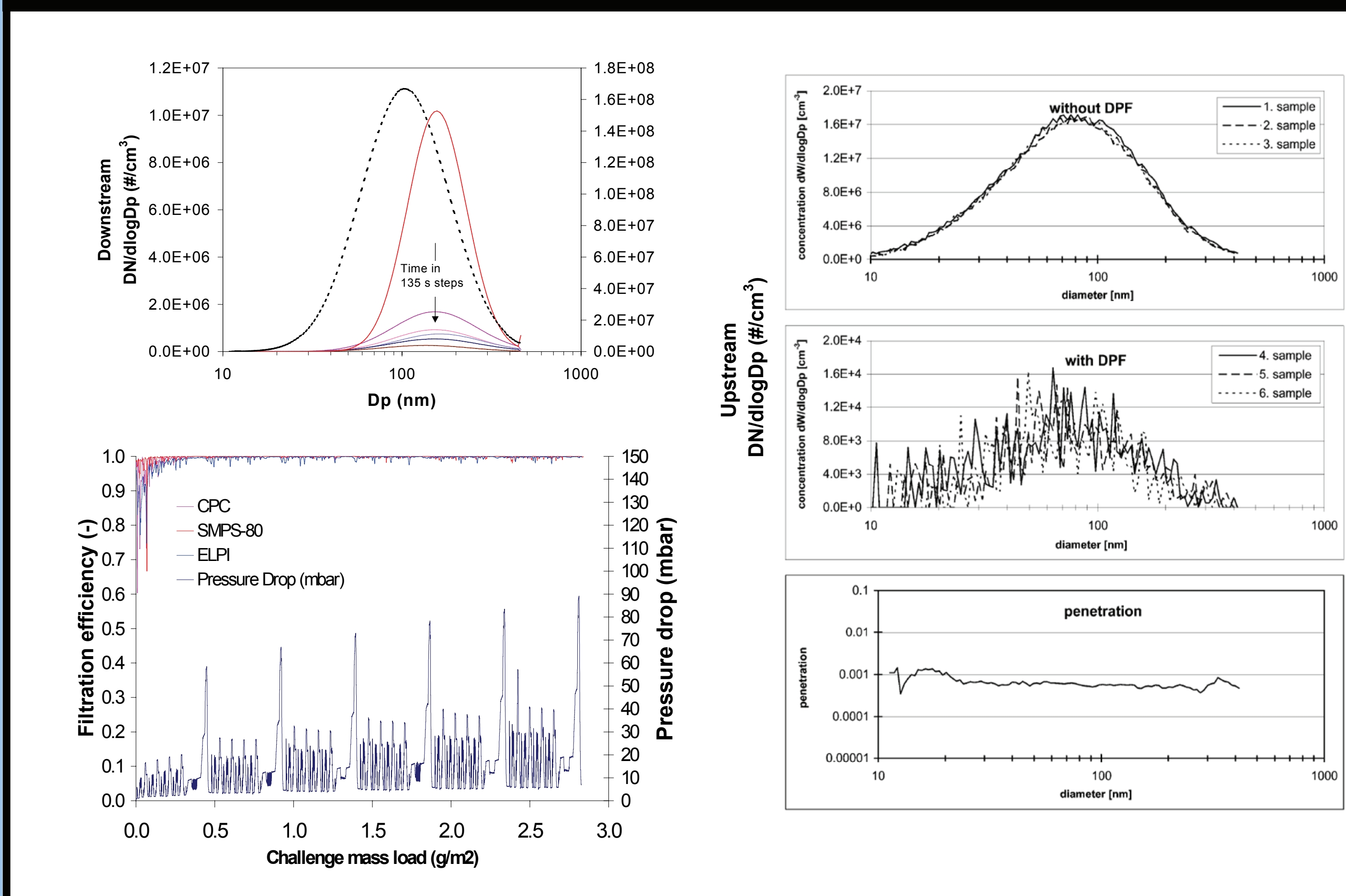
Bilal Zuberi, Ph.D.
GEO2 Technologies, Inc. Woburn, MA, USA
<http://www.geo2tech.com>

A new platform of advanced ceramic composite filter materials with cross-linked microstructure (CLM™) for diesel particulate matter and exhaust gas emission control has been developed by GEO2 Technologies. These materials extruded into wall-flow honeycomb filters exhibit high porosity (>60%), low backpressure, high nano-particle filtration efficiency, and robust thermo-mechanical strength.

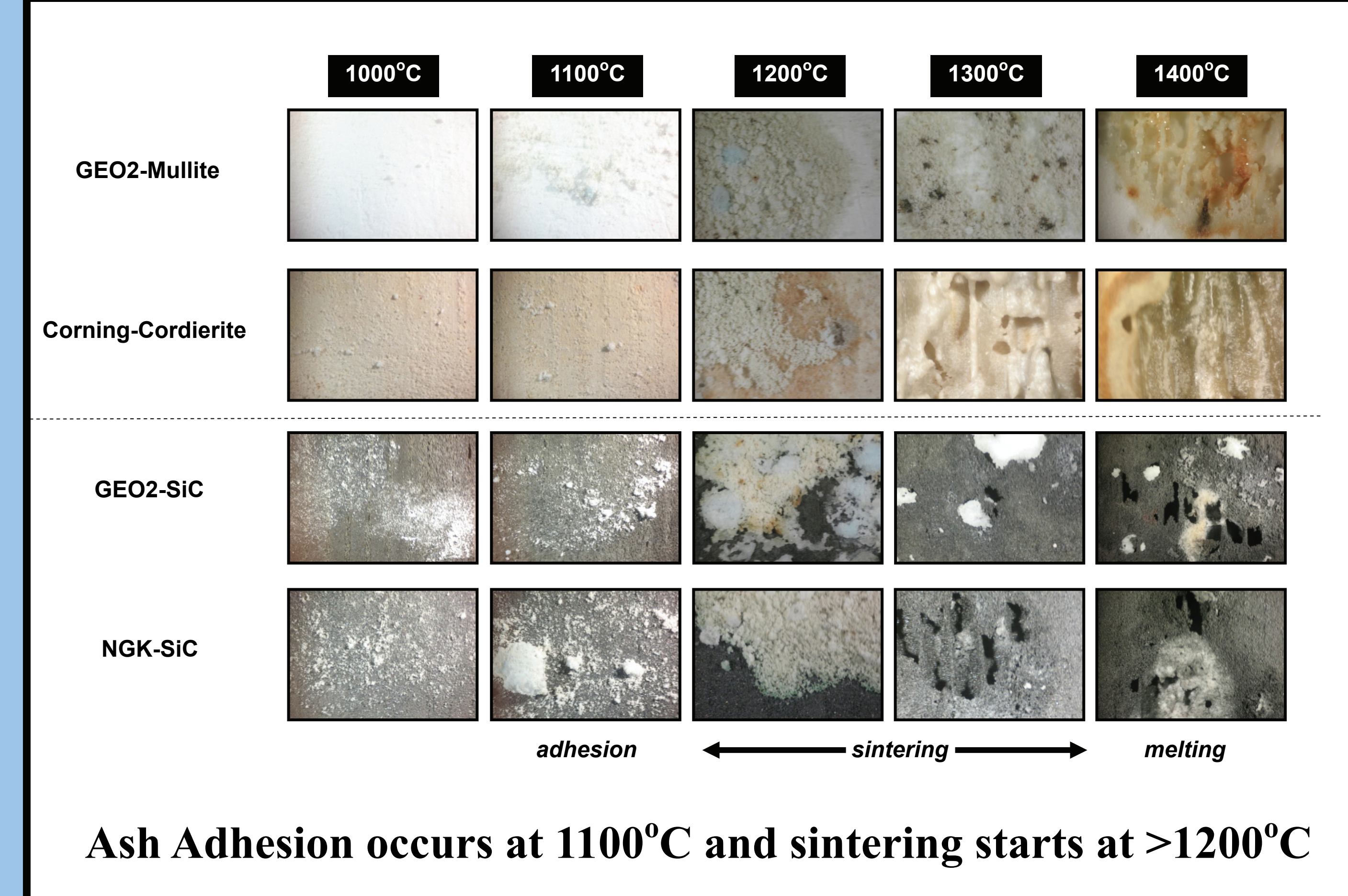
Introduction



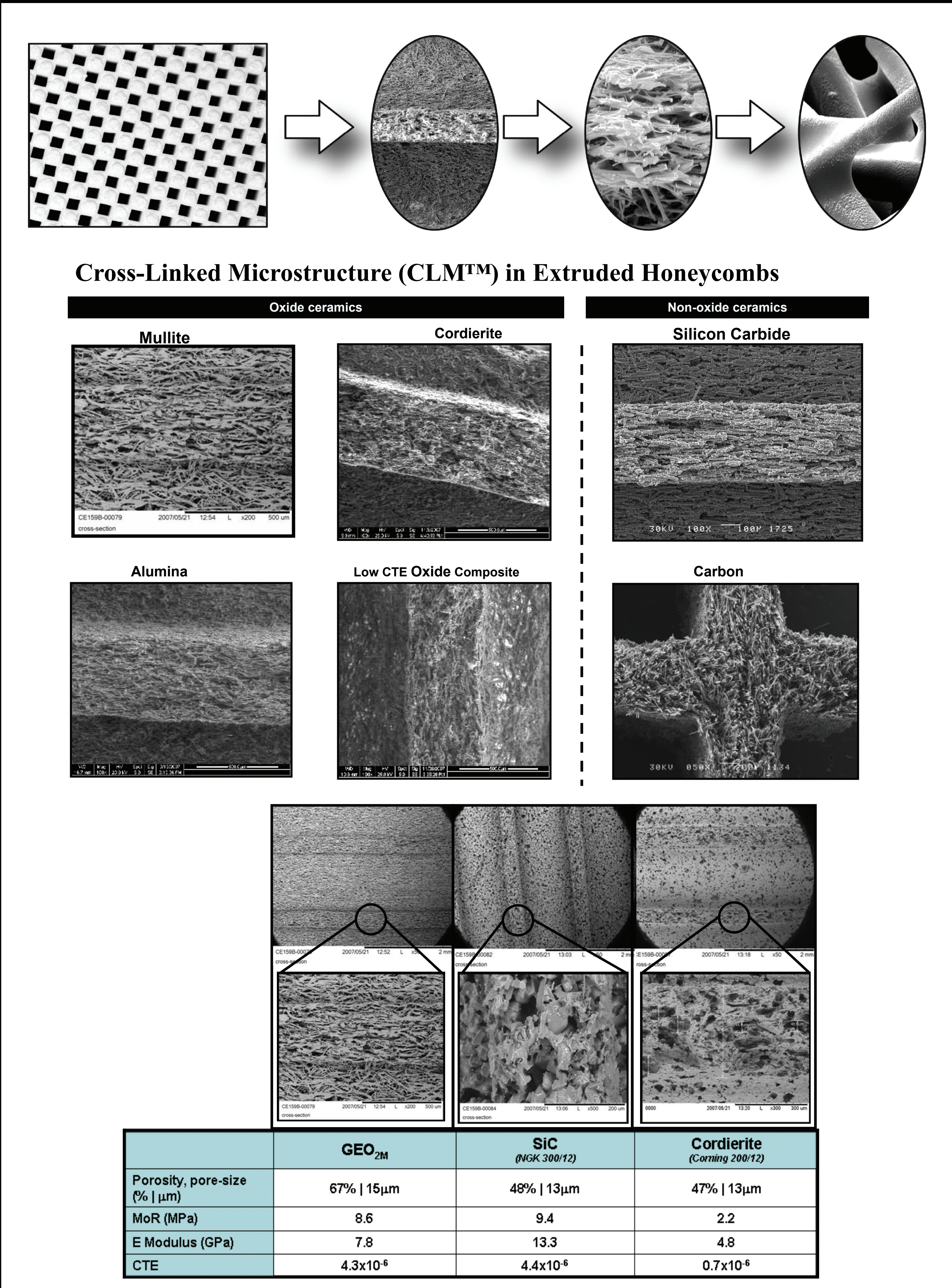
High Nano-particle Trapping Efficiency



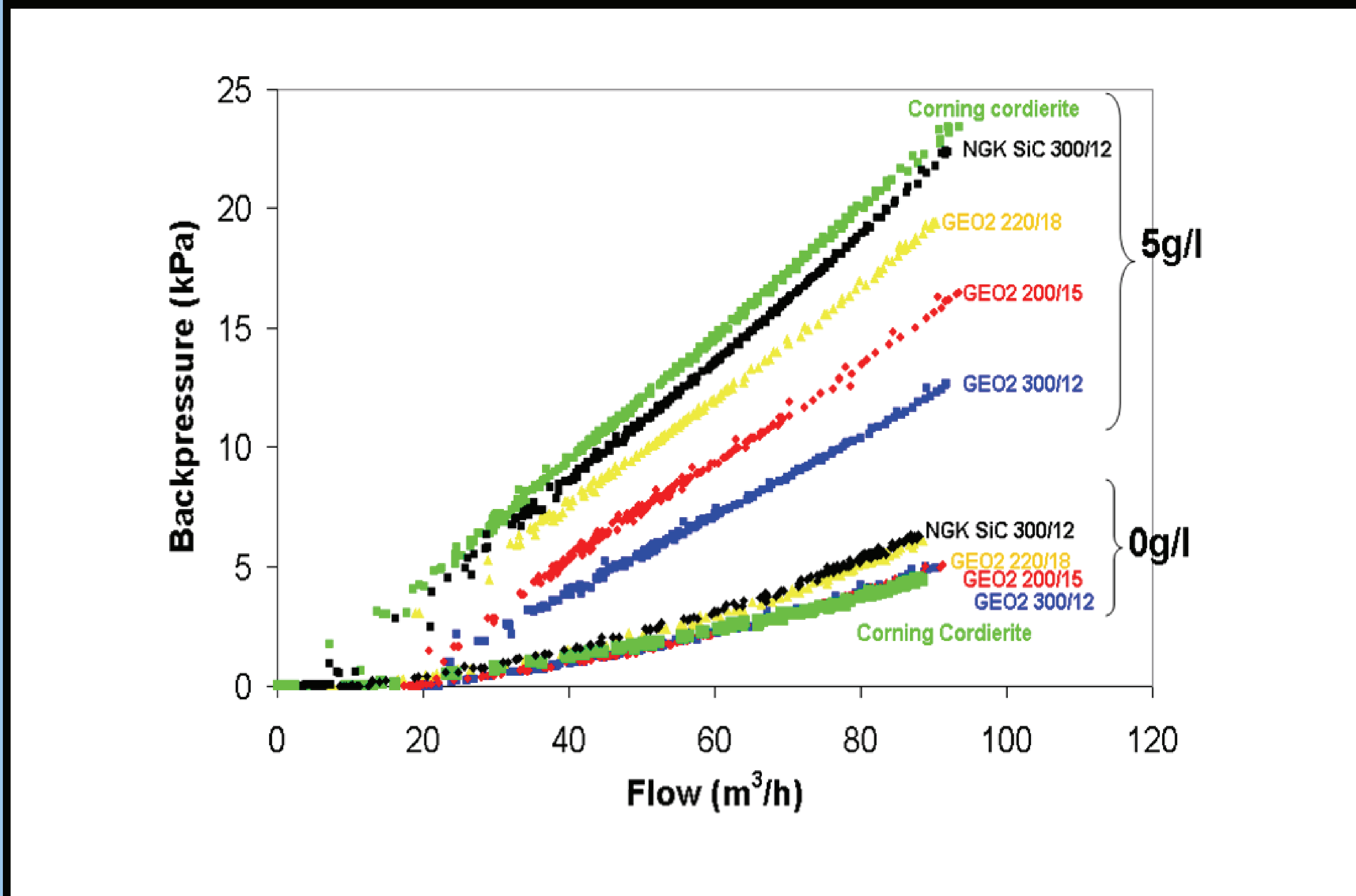
Resistance to Ash



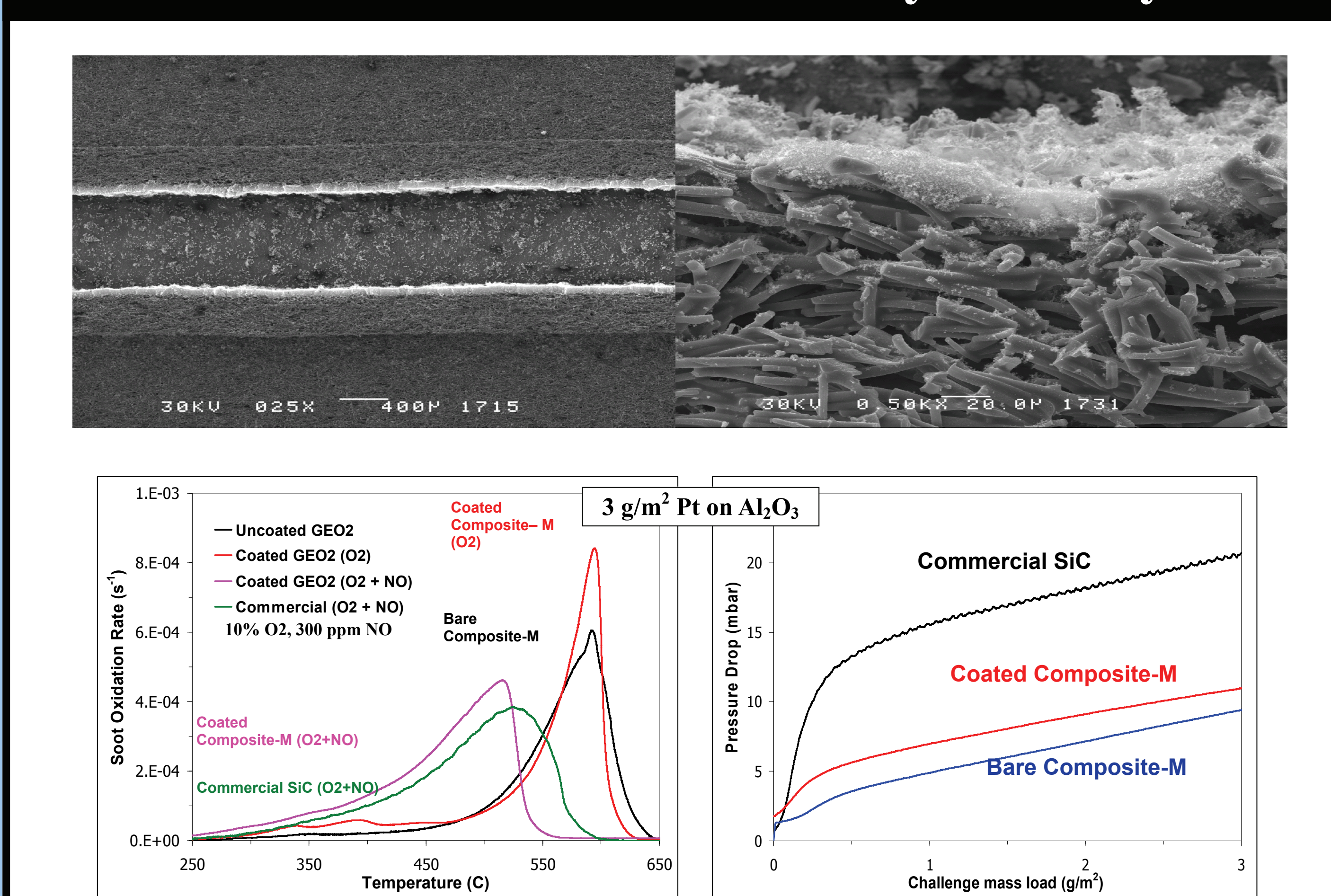
GEO2 Material Technology Platform



Low backpressure vs powder-based filters

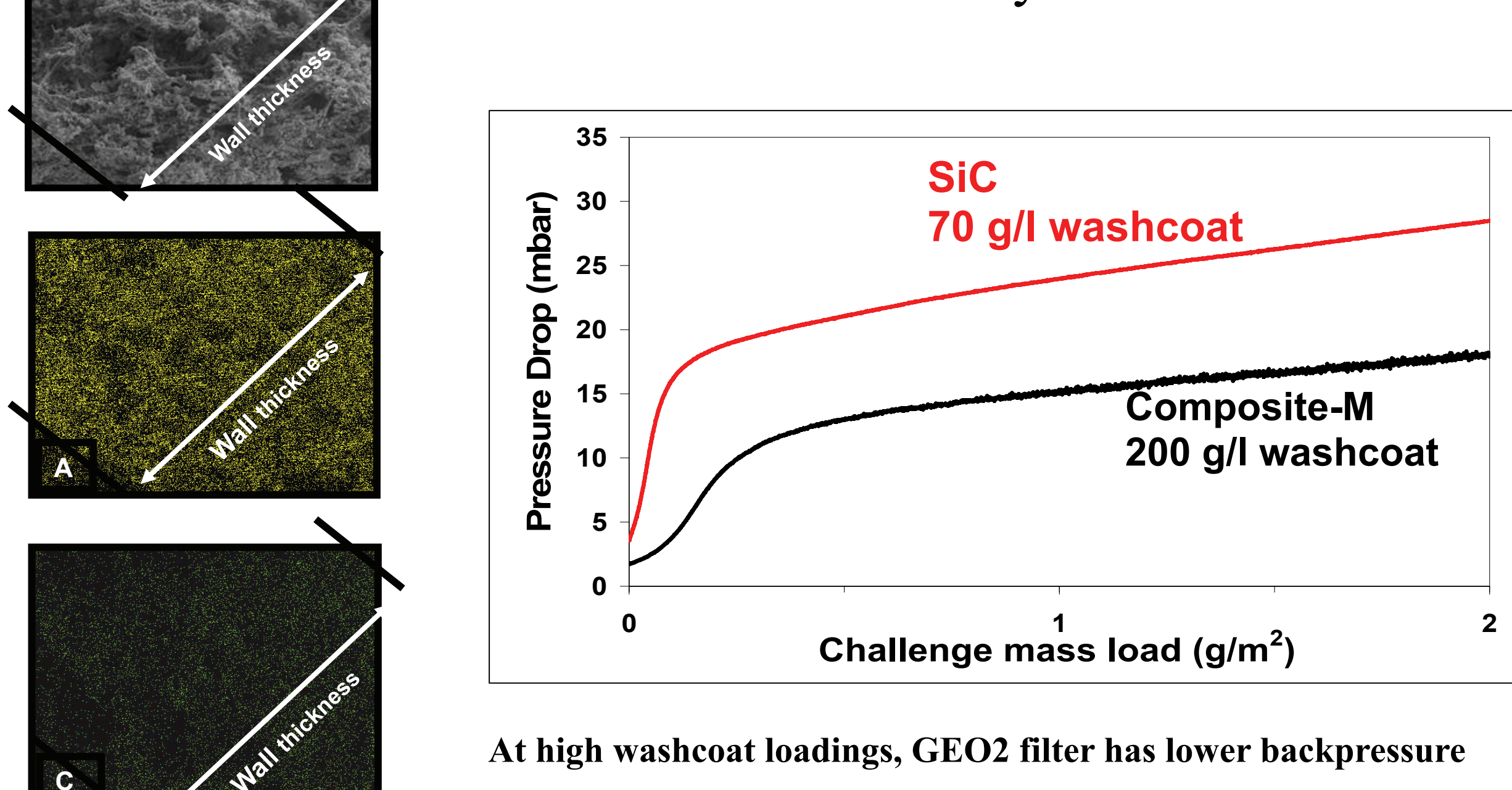


Enhanced contact and efficacy of catalyst



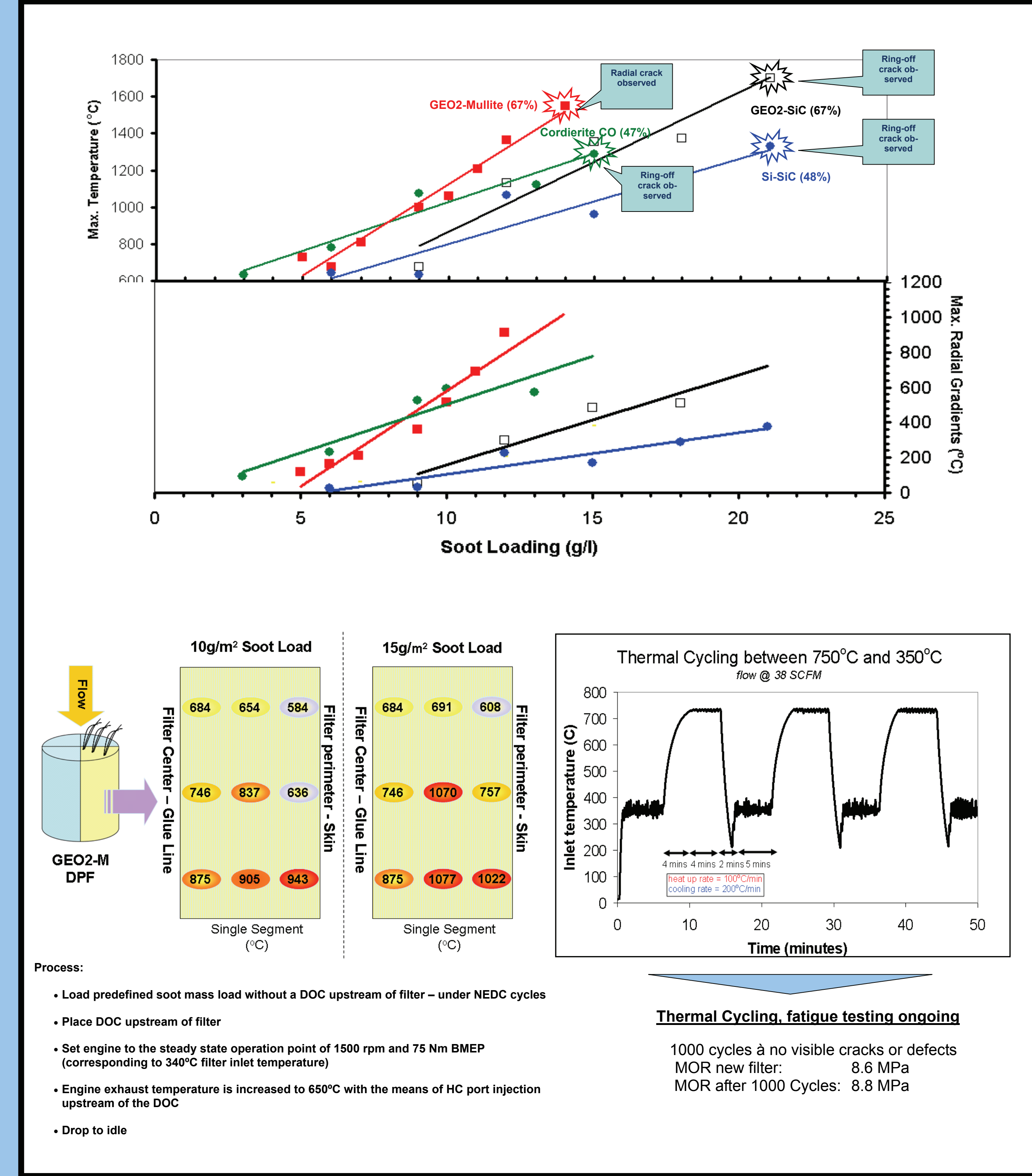
High porosity and uniform pore structure leads to efficient distribution of catalyst throughout wall. Useful for multi-functional/4-way catalysts

Base-metal oxide catalyst loaded on GEO2



At high washcoat loadings, GEO2 filter has lower backpressure

High Nano-particle Trapping Efficiency



Summary

Generic GEO₂ Process

Fibers + Bonding Chemistry + Extrusion Process = GEO₂ CLM

A new platform of Cross-Linked Microstructure (CLM™) materials has been developed to produce high porosity, low backpressure filters, with high nano-particle trapping efficiency. Mullite, Silicon Carbide and Cordierite chemistries are available. These materials are capable of supporting the high levels of washcoat loading that will be required by future emission control strategies.

For more information, please contact:
Bilal Zuberi, Ph.D.
Vice President, Product Development
bzuberi@geo2tech.com
<http://www.geo2tech.com>

A new ceramic material design parameter

